ADVANCES IN ATMOSPHERIC SCIENCES, VOL. 34, OCTOBER 2017, 1204–1218

• **Original Paper** •

Differences and Links between the East Asian and South Asian Summer Monsoon Systems: Characteristics and Variability

Ronghui HUANG[1,2,3], Yong LIU*[1], Zhencai DU[1], Jilong CHEN[1], and Jingliang HUANGFU[1]

[1]*Center for Monsoon System Research, Institute of Atmospheric Physics, Chinese Academy of Sciences, Beijing* 100190*, China*

[2]*State Key Laboratory of Numerical Modeling for Atmospheric Sciences and Geophysical Fluid Dynamics, Institute of Atmospheric Physics, Chinese Academy of Science, Beijing* 100029*, China*

[3]*Institute of Earth Sciences, University of Chinese Academy of Sciences, Beijing* 100049*, China*

(Received 17 January 2017; revised 11 April 2017; accepted 9 May 2017)

ABSTRACT

This paper analyzes the differences in the characteristics and spatio–temporal variabilities of summertime rainfall and water vapor transport between the East Asian summer monsoon (EASM) and South Asian summer monsoon (SASM) systems. The results show obvious differences in summertime rainfall characteristics between these two monsoon systems. The summertime rainfall cloud systems of the EASM show a mixed stratiform and cumulus cloud system, while cumulus cloud dominates the SASM. These differences may be caused by differences in the vertical shear of zonal and meridional circulations and the convergence of water vapor transport fluxes. Moreover, the leading modes of the two systems' summertime rainfall anomalies also differ in terms of their spatiotemporal features on the interannual and interdecadal timescales. Nevertheless, several close links with respect to the spatiotemporal variabilities of summertime rainfall and water vapor transport exist between the two monsoon systems. The first modes of summertime rainfall in the SASM and EASM regions reveal a significant negative correlation on the interannual and the interdecadal timescales. This close relationship may be linked by a meridional teleconnection in the regressed summertime rainfall anomalies from India to North China through the southeastern part over the Tibetan Plateau, which we refer to as the South Asia/East Asia teleconnection pattern of Asian summer monsoon rainfall. The authors wish to dedicate this paper to Prof. Duzheng YE, and commemorate his 100th anniversary and his great contributions to the development of atmospheric dynamics.

Key words: East Asian summer monsoon, South Asian summer monsoon, spatiotemporal variability, rainfall, water vapor transport

Citation: Huang, R. H., Y. Liu, Z. C. Du, J. L. Chen, and J. L. Huangfu, 2017: Differences and links between the East Asian and South Asian summer monsoon systems: Characteristics and variability. *Adv. Atmos. Sci.*, **34**(10), 1204–1218, doi: 10.1007/ s00376-017-7008-3.

1. Introduction

In the 100th anniversary of Prof. Duzheng YE (i.e. Tu-Cheng YEH), as one of his former students, I (Ronghui HUANG) and my coauthors wish to dedicate this study to commemorate this outstanding meteorologist and his substantial contributions to the development of the atmospheric sciences and the foundations of the modern era of this discipline in China. Accordingly, we begin with a brief summary of Prof. YE's research experience and achievements.

Prof. YE was without doubt one of the world's most outstanding meteorologists and, domestically, one of the major founders of modern-day atmospheric sciences in China. Over a more than 70-year research career he made many important contributions to the development of atmospheric sciences, including proposing the theory of energy dispersion of Rossby waves, establishing a theory of atmospheric general circulation over East Asia, initiating the study of Tibetan Plateau meteorology, proposing a scale theory regarding the adaptation process of atmospheric motion, and pioneering the new concept of adaptation to global warming (Yeh, 2008). To develop the atmospheric sciences in his home country, Prof. Ye left Chicago University for China in 1950. Subsequently, he invested considerable energy into improving and organizing the research activities of this discipline within the Chinese research community. Together with his colleagues (e.g. Profs. Shiyan TAO and Zhenchao GU), Prof. YE dedicated a great deal of effort into developing the study of atmospheric sciences in China, especially those related to East Asian general circulation. From the 1950s to the 1960s, Prof. YE systematically studied the characteristics and variabilities of East

* Corresponding author: Yong LIU
Email: liuyong@mail.iap.ac.cn

Asian general circulation, through observational and theoretical analyses, in cooperation with Profs. Shiyan TAO and Baozhen ZHU and others (staff members of the Section of Synoptic and Dynamic Meteorology, Institute of Geophysics and Meteorology, Academia Sinica, 1957, 1958a, 1958b; Ye and Zhu, 1958). The studies conducted by Profs. YE, TAO and colleagues showed that the seasonal variation of the general circulation over East Asia from winter to summer is very distinct and fairly abrupt (Ye et al., 1959). Moreover, they also pointed out that this abrupt change in planetary-scale circulation brings about the onset of the East Asian summer monsoon (EASM). This abrupt change in monsoon circulation was further demonstrated in the 1980s by Krishnamurti and Ramanathan (1982) and McBride (1987), in studies on the Indian summer monsoon and Australian monsoon.

Enlightened by the theory of atmospheric general circulation over East Asia proposed by Prof. YE, scientists have been able to carry out studies on the characteristics, causes and mechanisms of the spatiotemporal variabilities of the EASM system. It is known, for instance, that the EASM system has notable interannual and interdecadal variabilities and, owing to that, climatic disasters such as droughts and floods occur frequently in summer in China (Huang and Zhou, 2002; Huang et al., 2004, 2006a, 2007, 2008, 2011a; Huang, 2006). Indeed, since the 1980s, severe and frequent climatic disasters over large areas have caused vast amounts of damage to agricultural and industrial production in China (Huang et al., 1998a, 1999; Huang and Zhou, 2002; Wang and Gu, 2016). Therefore, it is of great importance to study the variability and possible causes of the EASM, as well as its links to nearby or remote climate systems.

The Asian monsoon region is one of several monsoon climate regions worldwide and, generally, it is considered to comprise two subcomponents (Webster et al., 1998; Ding et al., 2013)—namely, the East Asian and South Asian summer monsoons (hereafter referred to as the EASM and SASM, respectively). It has been documented by many studies that the characteristics of the EASM and SASM system are different (Tao and Chen, 1987; Huang et al., 1998b, 2012; Wang et al., 2001). For instance, the EASM has both tropical and subtropical characteristics because, not only it is influenced by the western Pacific subtropical high and the disturbances over the middle latitudes, but also by tropical circulation systems, such as Maritime Continent convection; whereas, the SASM only has tropical properties, such as the Mascarene high, Somali jet, and so on. However, the EASM and SASM systems also show links. For example, strong SASM flow delivers a large amount of water vapor into the EASM region from the Bay of Bengal, which can cause strong rainfall and severe floods in this region. Previous studies have also indicated the existence of a close relationship between the summer precipitation of the SASM and EASM (Guo and Wang, 1988; Guo, 1992; Kripalani and Singh, 1993; Kripalani and Kulkarni, 2001; Ding and Wang, 2005; Lin et al., 2016; Wu, 2002, 2017), although Wu (2017) pointed out that this relationship has become unstable and weakened since the late 1970s.

Because of the complexity of the EASM and SASM systems, the differences and links between them—in particular, with respect to the dominant modes of summertime rainfall and water vapor transport—are still not clearly understood. Accordingly, using long-term observational and reanalysis data, the present study aims to systematically investigate these issues. Specifically, we examine: (1) the differences in the characteristics of rainfall cloud systems and their association with the vertical shear of zonal and meridional circulations and the convergence of water vapor transport; (2) the differences in the spatiotemporal variabilities of summertime rainfall and water vapor transport between the EASM and SASM systems; and (3) the links between the two systems in terms of their spatiotemporal variabilities of summertime rainfall and water vapor transport.

The remainder of the paper is structured as follows: Section 2 details the datasets and methods used in the study. Section 3 describes the climatological characteristics of the rainfall and general circulation of the EASM and SASM, and highlights the differences between them. Sections 4 and 5 analyze the features and differences of the interannual and interdecadal variabilities of summer rainfall in the two monsoon regions. The links in terms of summer rainfall variability between the EASM and SASM are explained in section 6 and, finally, a conclusion and further discussion are provided in section 7.

2. Data and methodology

The data used in the present work are as follows: (1) NCEP–NCAR reanalysis data, covering the period from 1961 to 2014 (Kalnay et al., 1996); (2) Tropical Rainfall Measuring Mission (TRMM) Precipitation Radar Rainfall L3 monthly data, version 7, with a $0.5^\circ \times 0.5^\circ$ mesh (TRMM_3A25), covering the period from 1998 to 2015 (TRMM, 2011); (3) Precipitation data from the Climate Research Unit (CRU) TS3.23 precipitation dataset, with a $0.5^\circ \times 0.5^\circ$ horizontal resolution in the Asian region from 1961 to 2014 (Harris et al., 2014); (4) and precipitation data from 597 observational stations in China for the period 1961 to 2014, archived and updated by the China Meteorological Administration (http://data.cma.cn/data/cdcdetail/dataCode/SURF_CLI_CHN_MUL_DAY_V3.0.html).

The present work employs empirical orthogonal function (EOF) analysis to investigate the spatiotemporal features of summer (June–July–August) precipitation in the EASM and SASM regions, wherein the first two leading modes of summer rainfall in the two monsoon regions are adopted, respectively. Based on the method of North et al. (1982), the first two modes of summer rainfall in each monsoon region are completely separated. The present work also uses correlation analysis and regression analysis and the two-tailed Student's *t*-test to detect the statistical significance of a signal, and the effective degrees of freedom is calculated according to the method of Davis (1976). In addition, to discuss the interdecadal variability of summer rainfall in the two monsoon regions, we adopt a 9-yr running mean method to obtain the interdecadal component of the summer precipitation.

The atmospheric water vapor transport and its convergence are estimated based on the following expressions. The vertically integrated water vapor transport flux vector, $\boldsymbol{Q} = (Q_\lambda, Q_\varphi)$, and its zonal and meridional components, Q_λ and Q_φ, are described as follows:

$$Q_\lambda = \frac{1}{g}\int_{300}^{p_0}(qu)dp\ ; \tag{1}$$

$$Q_\varphi = \frac{1}{g}\int_{300}^{p_0}(qv)dp\ . \tag{2}$$

Here, g is the gravitational acceleration; q is the specific humidity; and u and v represent the zonal and meridional winds, respectively. For the sake of simplicity and to avoid the problem of data limitation (the top level in the specific humidity field only reaches up to 300 hPa), thus, the integration is from the bottom level (p_0 = 1000 hPa) and to the top level (300 hPa).

In a spherical coordinate system, the divergence of water vapor transport fluxes, $\nabla\cdot\boldsymbol{Q}$, can be calculated using the following formula:

$$\nabla\cdot\boldsymbol{Q} = \frac{1}{a\cos\varphi}\left(\frac{\partial Q_\lambda}{\partial\lambda} + \frac{\partial Q_\varphi\cos\varphi}{\partial\varphi}\right), \tag{3}$$

where (λ,φ) represents the longitude and latitude, respectively, and a is the Earth's radius. Furthermore, if topography is not considered, $\nabla\cdot\boldsymbol{Q}$ can be divided into two parts (thermal and dynamic components), as follows:

$$\begin{aligned}\nabla\cdot\boldsymbol{Q} &= \frac{1}{g}\int_{300}^{p_0}\nabla\cdot(\boldsymbol{V}q)dp\\ &= \frac{1}{g}\int_{300}^{p_0}\boldsymbol{V}\cdot\nabla q dp + \frac{1}{g}\int_{300}^{p_0}q(\nabla\cdot\boldsymbol{V})dp.\end{aligned} \tag{4}$$

The first of the two terms on the right-hand side of Eq. (4) is the quantity due to moisture advection (i.e. the thermal component), and the second is the quantity due to divergence of the wind field (i.e. the dynamic component). Based on the first part of Eq. (4), moist advection can cause local convergence of the water vapor flux, but dry advection leads to local divergence of the water vapor flux. As for the second part, local wind circulation convergence benefits local convergence of the water vapor flux, and vice versa.

3. Rainfall and circulations of the EASM and SASM regions: climatological characteristics and differences

As mentioned, the EASM system is a relatively independent subtropical monsoon circulation system and has different horizontal circulations from the SASM system (Tao and Chen, 1987). However, importantly, differences between the two monsoon systems may also exist in terms of the vertical structure of the zonal and meridional circulations, which may further lead to differences in their rainfall cloud systems and water vapor transport. Therefore, the climatological characteristics of the two regions' rainfall cloud systems, vertical structure of horizontal circulations, and water vapor transport, and their differences, are explored in this section.

3.1. *Rainfall cloud systems*

Using the TRMM_3A25 precipitation data, the distribution of the ratio of rainfall due to convective and stratiform cloud systems to total rainfall over the Asian summer monsoon region is analyzed. As shown in Fig. 1, the rainfall ratio related to convective cloud systems in the EASM region decreases with latitude, with the value reaching 50% in the low latitudes to the south of 25°N (Fig. 1a). Meanwhile, the rainfall ratio related to stratiform cloud systems exhibits the opposite feature, increasing from low to high latitudes, with the value increasing to 65% to the north of 25°N (Fig. 1b). Specifically, the rainfall over South China due to convective and stratiform cloud systems is comparable, which agrees with the findings of Fu et al. (2003) and Liu and Fu (2010). These features suggest that summertime rainfall cloud systems over the EASM region are a mix of stratiform and convective cloud systems—something that may lead to difficulty in parameterizing cumulus cloud when numerically modeling the EASM system (Cheng et al., 1998).

As for the SASM region, the ratio of the rainfall induced by convective/stratiform cloud systems to total rainfall is uniformly spread over continental India. Furthermore, the rainfall induced by convective cloud systems contributes more than 60% of the total rainfall (Fig. 1a), while the ratio of the rainfall induced by stratiform cloud systems to total rainfall is about 35% over India (Fig. 1b). This indicates that the summertime rainfall cloud systems over the SASM region are dominated by convective cloud, which is different to the situation over the EASM region.

3.2. *Zonal and meridional circulation*

As mentioned, the vertical structure of the horizontal circulations over the EASM and SASM regions are different, which may be responsible for their differences in monsoon rainfall cloud systems. Thus, the differences in the vertical shear of zonal and meridional circulations between these two monsoon regions are investigated in this part of the study. Figure 2 displays the vertical distribution of the climatological mean zonal and meridional wind averaged over the domains (20°–45°N, 100°–140°E) and (0°–25°N, 60°–100°E), representing the EASM and SASM regions, respectively. As shown in Fig. 2a, during boreal summer, the climatological mean zonal circulation over the EASM region is characterized by westerly wind throughout the troposphere in the vertical direction, showing obvious vertical westerly shear. This may be unfavorable for the intensification of convective cloud systems, but favorable for the formation of stratiform cloud systems. Thus, there is a mix of stratiform and convective cloud systems in the EASM region. However, the SASM system belongs purely to the tropical monsoon, with notable westerly wind prevailing in the lower troposphere below 500 hPa and easterly wind in the mid/upper troposphere (Fig. 2b), showing strong vertical easterly shear. But, the wind speed is weaker than that in the EASM region. The low-level west-

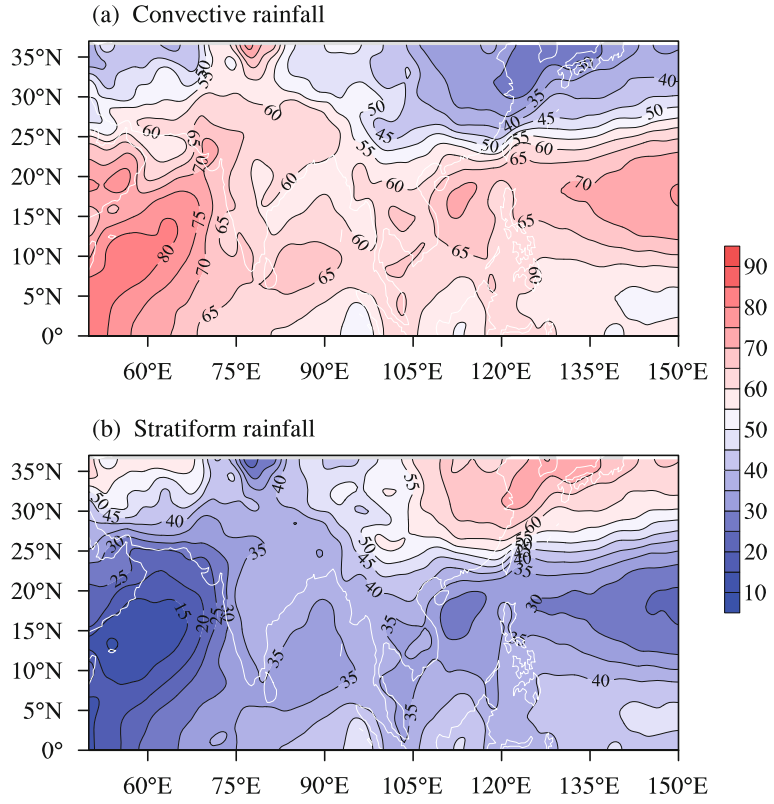

Fig. 1. Climatological-mean distributions of summertime rainfall (%) due to (a) convective rainfall and (b) stratiform rainfall, for 17 summers during 1998–2014, based on TRMM data.

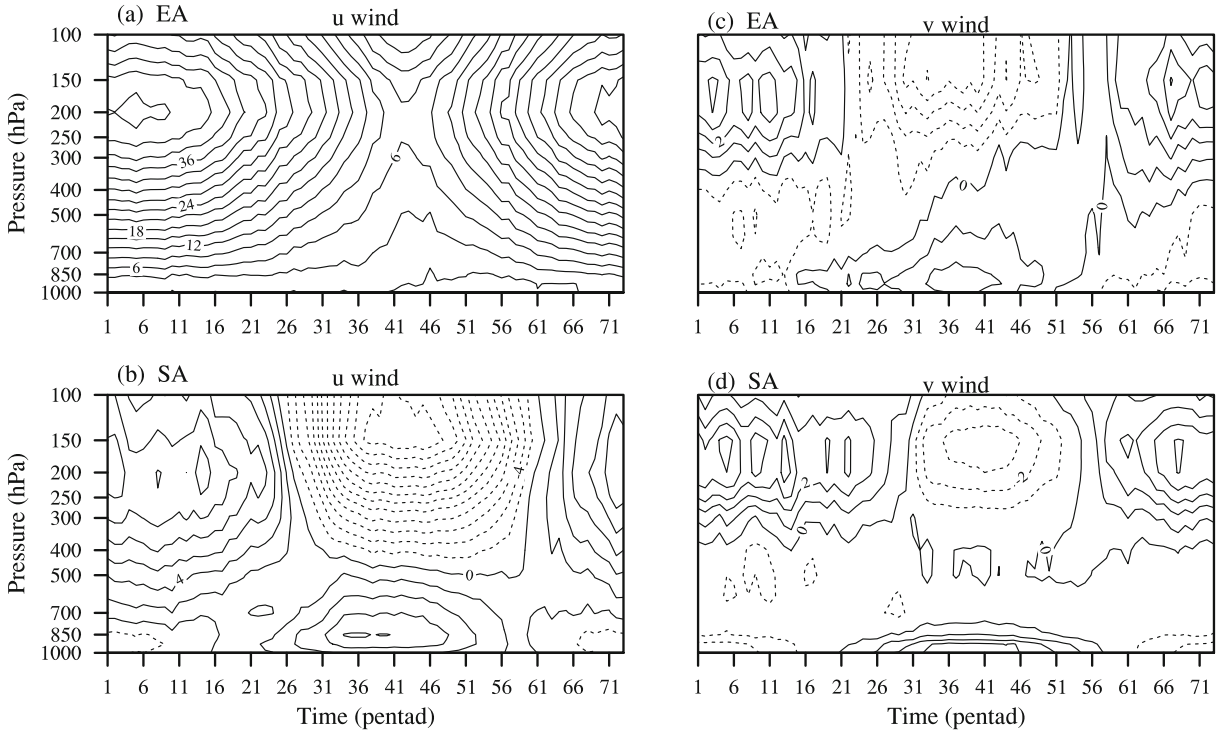

Fig. 2. Time–height cross section of climatological (a, b) zonal and (c, d) meridional winds, averaged for 26 summers during 1979–2014 over (a, c) East Asia (20°–45°N, 100°–140°E) and (b, d) South Asia (0°–25°N, 60°–100°E). Solid and dashed lines indicate westerly/southerly and easterly/northerly winds, respectively. Units: m s^{-1}.

erly wind and vertical easterly shear may be favorable for the intensification of convective activity in the SASM region, resulting in the monsoon rainfall mainly triggered by convective cloud systems in this region (Halverson et al., 2002).

As for the meridional circulation, significant meridional flow with low-level southerly and high-level northerly prevails in the EASM region (Fig. 2c), featuring strong vertical northerly shear and suggesting it is composed of tropical and subtropical summer monsoon characteristics. In contrast, the meridional circulation in the SASM region is characterized by low-level southerly flow (below 800 hPa, approximately) and strong upper-level northerly flow (Fig. 2d). Furthermore, it is clear that southerly wind prevails over larger ranges in the EASM region compared with the SASM region—a situation that is the reverse for the northerly flow. This shows that the vertical northerly shear of meridional circulation over the SASM region is stronger than that over the EASM region.

As indicated above, there are obvious differences in the vertical shear of horizontal circulation between the EASM and SASM systems, which may lead to their differences in monsoon rainfall cloud systems. This suggests that different ways can be used to measure the strength and variability of the two monsoon systems and, as such, different monsoon indices have been defined for the two monsoon systems. For example, Huang (2004) and Zhao et al. (2015) defined East Asia–Pacific (EAP) indices that measure the strength of the EASM system using the 500-hPa geopotential height and the zonal wind at 200 hPa, respectively. Meanwhile, Wang and Fan (1999) and Webster and Yang (1992) defined the strength of the SASM system using the zonal wind in the lower troposphere and the difference in the zonal wind between the upper and lower troposphere, respectively.

3.3. *Water vapor transport*

Water vapor transport and its convergence are of great importance to local rainfall variation. As analyzed above, the horizontal and vertical features of the circulation over the EASM and SASM regions show significant differences, and this may lead to differences in the characteristics of water vapor transport and its convergence over the two monsoon regions. Therefore, the water vapor transport, its convergence, and associated thermal and dynamical components, are analyzed in this subsection.

Figure 3a displays the climatological mean distribution of summertime water vapor transport fluxes over the EASM and SASM regions during 1979–2014, calculated based on Eqs. (1) and (2). Clearly, the distribution of water vapor transport flux is significantly different in the two monsoon regions. There are three sources for water vapor transport in the

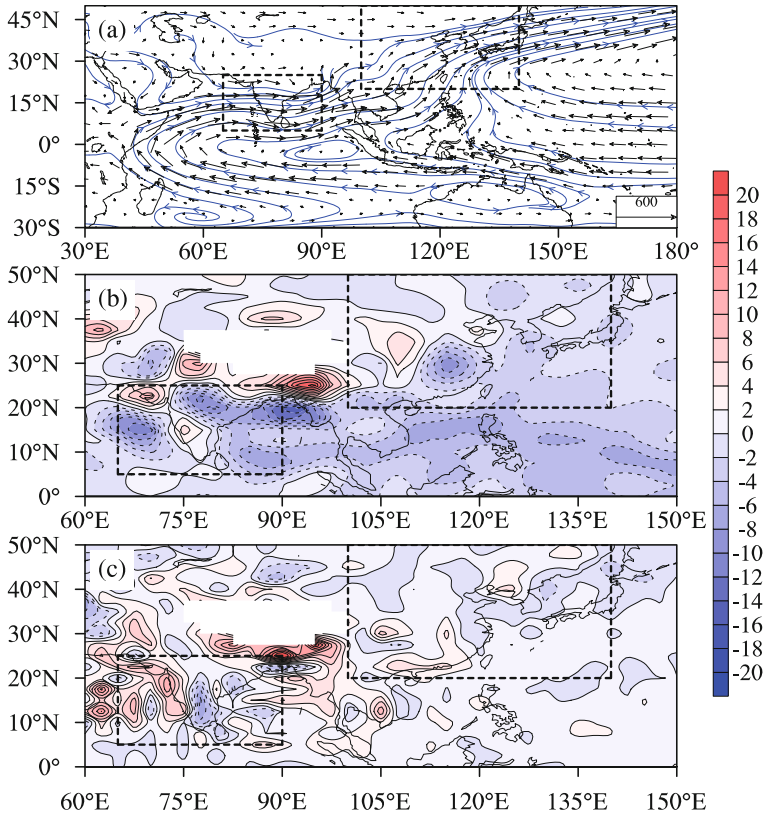

Fig. 3. Climatological mean distribution of vertically integrated summertime water vapor transport fluxes (a), and its divergence due to (b) wind divergence and (c) moisture advection, averaged for 26 summers during 1979–2014. The EASM (right-hand box) and SASM (left-hand box) regions are plotted. The unit for (a) is kg m^{-1} s^{-1}, and that for (b) and (c) is kg m^{-2} s^{-1}.

EASM region: from the Bay of Bengal, the South China Sea, and the tropical western Pacific. Owing to the abundant water vapor delivered by the summer monsoon flow from these source regions, the meridional water vapor transport fluxes are significant over South China and the Yangtze River valley. However, with respect to the SASM region, the zonal transport fluxes of water vapor are notably larger than the meridional transport fluxes.

Figures 3b and c show the climatological thermal and dynamical contributions to the divergence of the water vapor transport flux, i.e. by moisture advection and wind divergence, respectively. It is clear that, in the EASM region, the southern part is dominated by the dynamical contribution of wind divergence, while the northern part is dominated by moisture advection. As for the SASM region, the contribution of the wind divergence component is relatively smaller than that of moisture advection, especially over the northern India. By contrast, both the dynamical and thermal contributions are relatively smaller in the EASM region than in the SASM region.

From the above analyses, we can conclude that there are remarkable differences in the rainfall cloud systems, vertical structure of horizontal circulation, and water vapor transport, of the EASM and SASM regions, and that these are responsible for their differences in monsoon rainfall characteristics during boreal summer.

4. Interannual variability of summertime rainfall in the EASM and SASM regions and their differences

As indicated in the previous section, the climatological features of the rainfall cloud systems, circulation, and water vapor transport in the EASM and SASM regions are different from one another, making it conceivable that the spatiotemporal variability of the summer rainfall in the two monsoon regions may also be different. Therefore, using the observational station and gridded data and the EOF method, this section analyzes the spatiotemporal variability of the summer rainfall in the EASM and SASM regions.

4.1. *Characteristics of the interannual variability of summertime rainfall in the EASM region*

Figures 4 and 5 depict the spatial distributions and corresponding time-coefficient series and their wavelet analyses for the two leading modes of summertime rainfall anomalies in eastern China, respectively. As shown in Fig. 4a, the first leading mode characterizes a meridional tripole pattern in eastern China, and exhibits an obvious interannual variability with a period of 2–3 years, i.e. quasi-biennial oscillation, before the early 1990s, which may be influenced by the interannual variability of the thermal states of the western Pacific warm pool (Huang et al., 2006b, 2006c). Meanwhile, the interdecadal variability of the first leading mode is also remarkable from the late 1970s (Figs. 4b and c). As for the second leading mode, it features a meridional dipole pattern in eastern China (Fig. 5a); plus, it also exhibits an obvious interannual variability with a period of 2–3 years, especially from the mid-1960s to the late-1970s and from the early-1990s to the late-1990s, while its variability shifts and has a period of 3–8 years from the late-1990s onwards (Figs. 5b and c). Therefore, the interannual variability of summertime rainfall in the EASM region is unstable and characterized by multiple modes with an interdecadal change from the late-1990s. Accordingly, climatic disasters have occurred frequently in China (Huang et al., 2008, 2011b).

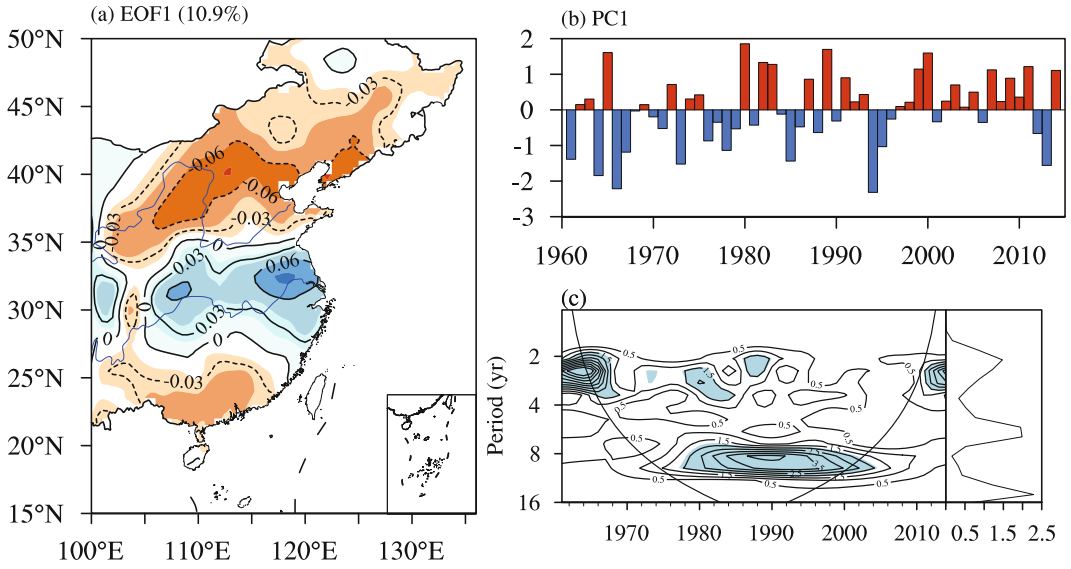

Fig. 4. Spatial distribution of the first leading mode of summer rainfall anomalies in eastern China (a), and the (b) corresponding time-coefficient series and (c) wavelet analysis for 1961–2014. Solid and dashed lines in (a) indicate positive and negative signals, respectively. EOF1 explains 10.9% of the total variance. Shading in (c) depicts the power significant beyond the 95% confidence level.

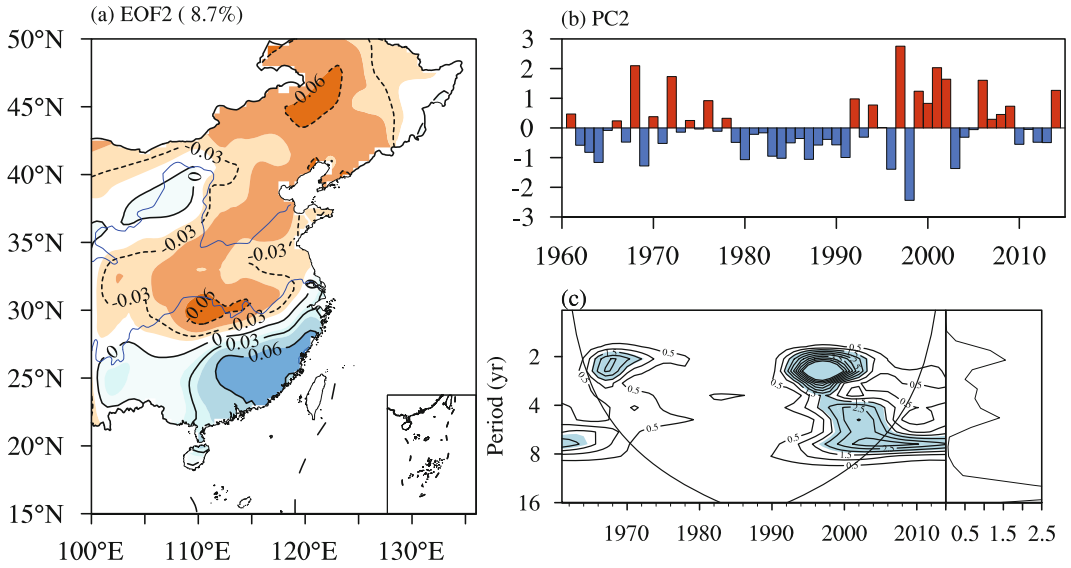

Fig. 5. As in Fig.4 but for the second mode, which explains 8.7% of the variance.

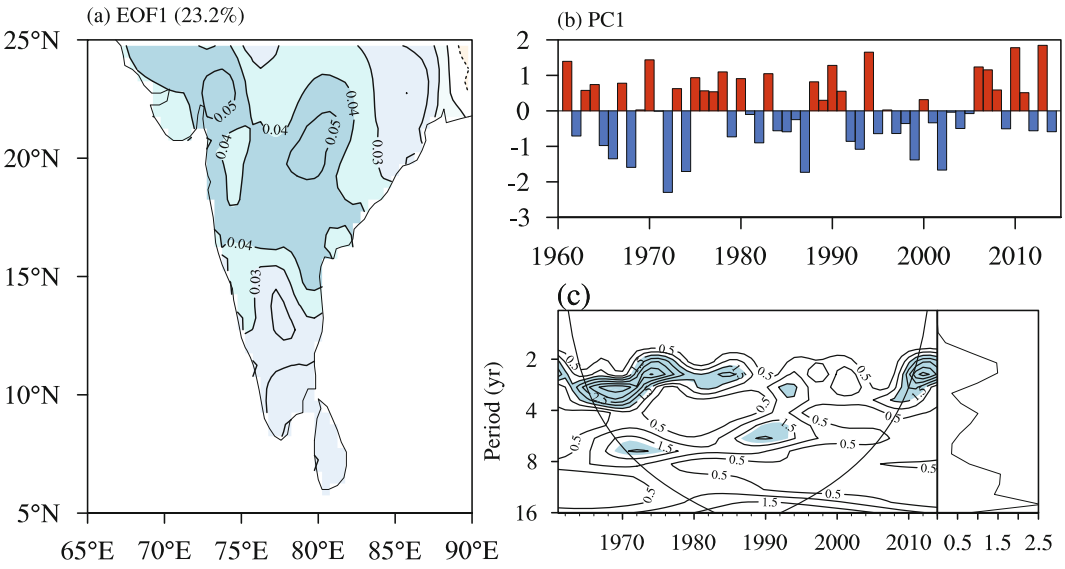

Fig. 6. As in Fig. 4 but for summer rainfall in the SASM (Indian) region. EOF1 explains 23.2% of the variance.

4.2. *Characteristics of the interannual variability of summertime rainfall in the SASM region*

For comparison, the spatiotemporal variability of summertime rainfall in the SASM region is also analyzed. Figure 6 depicts the spatial distribution, corresponding time-coefficient series and wavelet analyses of the first mode of summertime rainfall in the SASM region for 1961–2014. The first mode of summertime rainfall anomalies in the SASM region explains about 23.2% of the total variance and exhibits a uniform pattern in its spatial distribution. Additionally, it reveals a notable interannual variability with quasi-biennial oscillation (Figs. 6b and c), which agrees with the findings of Yasunari and Suppiah (1988). As shown in Fig. 7a, the second mode of summertime rainfall in the SASM region accounts for about 15.0% of the total variance and displays a meridional dipole pattern from the south to the north of India. The interannual variability of the second mode is also significant, with quasi-biennial oscillation during the periods from the mid-1970s to the mid-1980s and from the mid-1990s to the late-2000s, and 4–5 years during the period from the mid-1980s to the mid-1990s (Figs. 7b and c).

4.3. *Differences in the characteristics of the interannual variability of summertime rainfall in the EASM and SASM regions*

From the above analyses, a quasi-biennial oscillation of summertime rainfall appears in both the EASM and SASM region. This is consistent with Ding (2007), who pointed out that quasi-biennial oscillation may be a leading mode of the Asian summer monsoon system, including the EASM and SASM systems. However, comparing Fig. 3a with Fig. 6a, an obvious difference is apparent in terms of their spatial dis-

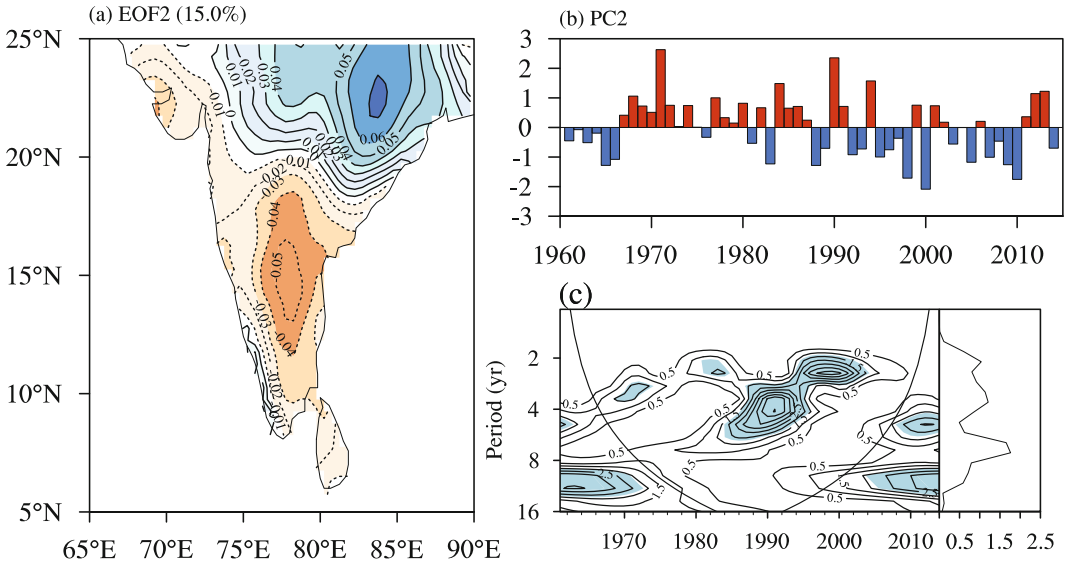

Fig. 7. As in Fig. 6 but for the second mode, which explains 15.0% of the variance.

tributions. The spatial distribution of the first mode of summertime rainfall anomalies in the EASM region exhibits a meridional tripole pattern, whereas it exhibits a uniform pattern in the SASM region.

5. Interdecadal variability of summertime rainfall in the EASM and SASM regions and their differences

From section 4 we can state that, in addition to significant interannual variability, the summertime rainfall in the EASM and SASM regions reveal notable interdecadal variabilities. Huang et al. (1999) pointed out that, during the late-1970s to early-1990s, summer rainfall in North China decreased sharply, causing prolonged and severe droughts in the region, but the opposite situation occurred in the Yangtze River and Huaihe River valley regions. Recently, several studies have revealed that EASM rainfall also experienced a significant interdecadal change in the early-1990s (Kwon et al., 2007; Ding et al., 2008, 2009; Wu et al., 2010; Zhang, 2015), and in the late-1990s (Liu et al., 2011; Huang et al., 2011a,b, 2013). To compare the interdecadal variability of summertime rainfall between the EASM and SASM regions, 9-yr running mean summertime precipitation data for the two regions, along with the EOF method, are used.

5.1. *Characteristics of the interdecadal variability of summertime rainfall in the EASM region*

As shown in Fig. 8a, the first mode of the 9-yr running mean summertime rainfall in the EASM region, which explains 26.1% of the total variance, exhibits a notable meridional dipole structure, i.e. a south–north oscillation pattern. Furthermore, the corresponding time coefficients are positive during the period from the mid-1960s to the early-1990s (Fig. 8b) and, in combination with Fig. 8a, the summertime rainfall anomalies during this period feature a negative–positive meridional dipole pattern from the south to the north of eastern China, with negative anomalies in South China, the Yangtze River and Huaihe River valleys, and positive anomalies in North China. However, the opposite structure appears in this region from the early-1990s; the distribution of summertime rainfall anomalies exhibits a positive–negative meridional dipole pattern from the south to the north of eastern China.

As for the second mode of the interdecadal variability of the summer rainfall in the EASM region, it explains 19.2% of the variance and exhibits a meridional tripole pattern in its spatial distribution (Fig. 8c). The time coefficients shown in Fig. 8d are negative from the mid-1960s to the late-1970s and, corresponding to the spatial feature in Fig. 8c, it reveals the summertime rainfall anomalies during this period to be positive in North and South China and negative in the Yangtze River and Huaihe River valleys. Comparing Figs. 8d and b, we can see that the time coefficients of EOF2 are much larger than those of EOF1 prior to the 1980s. Thus, the distribution of summertime rainfall anomalies presents a positive–negative–positive meridional tripole pattern during this period. Also, from the late-1970s to early-1990s, the time coefficients of EOF2 change from negative to positive and, in combination with its spatial distribution shown in Fig. 8c, it can be seen that the summertime rainfall decreases in North and South China and increases in the Yangtze River and Huaihe River valleys, i.e. the distribution of summertime rainfall anomalies presents a negative–positive–negative meridional tripole pattern from the south to the north of eastern China, which is opposite to the situation in the previous period. As for the period from the early- to the late-1990s, although the time coefficients of EOF2 (Fig. 8d) are still positive, those of EOF1 become negative and larger than those of EOF2. In combination with Figs. 8a and c, the distribution of summertime rainfall anomalies presents an above-normal

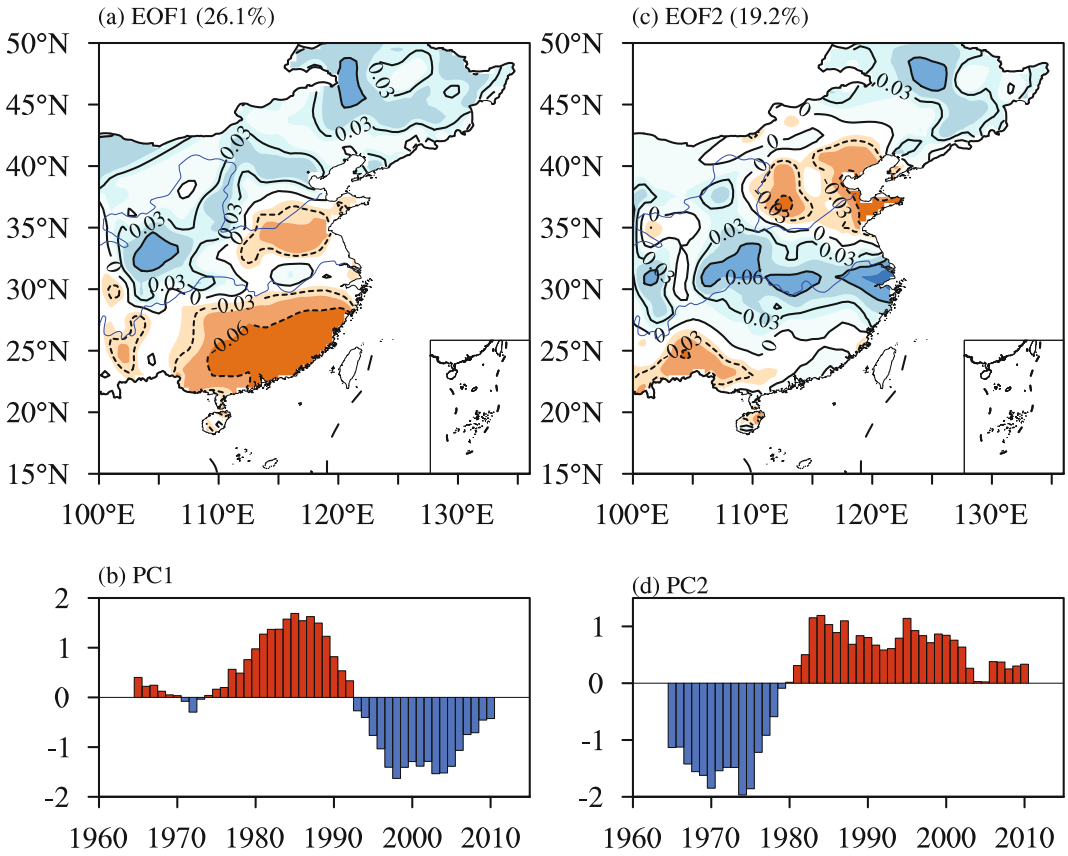

Fig. 8. As in Fig. 4 but for the first two leading modes of summer rainfall in eastern China on the interdecadal timescale: (a, c) spatial distribution; (b, d) corresponding time-coefficient series. EOF1 and EOF 2 explain 26.1% and 19.2% of the total variance, respectively.

pattern over the whole region, except for the northern area of North China. Also, since the negative time coefficients of EOF1 become larger from the late-1990s, the distribution of summertime rainfall anomalies presents a positive–negative meridional dipole pattern from the south to the north of eastern China—namely, a "south-flood–north-drought" pattern.

Moreover, to display the characteristics of the interdecadal variability even more clearly, we explore the features of the 9-yr running mean summertime rainfall anomalous percentages zonally averaged over the domain 100°–120°E. As shown in Fig. 9a, during the period from the mid-1960s to the late-1970s, the distribution of rainfall anomalies exhibits a positive–negative–positive meridional tripole pattern from the south to the north in eastern China. Furthermore, an opposite anomaly distribution, with a negative–positive–negative meridional tripole pattern, appears in eastern China during the period from the late-1970s to the early-1990s. As for the period from the early- to late-1990s, the rainfall anomalies in eastern China show a uniformly above-normal pattern, except in the Huaihe River valley. Meanwhile, from the late-1990s, the distribution of summertime rainfall anomalies presents a positive–negative meridional dipole pattern from the south to the north in eastern China. These features are coherent with the interdecadal variability described by the leading modes of the 9-yr running mean summertime rainfall in the EASM region. In addition, the positive and negative anomalies of summertime rainfall in eastern China indicate an anomalous signal moving from the north to the south on the interdecadal timescale (Fig. 9a).

5.2. *Characteristics of the interdecadal variability of summertime rainfall in the SASM region*

For comparison, the interdecadal variability of summertime rainfall in the SASM region is analyzed using the CRU precipitation data for 1961–2014. As shown in Fig. 10a, the first mode of summertime rainfall in the SASM region explains 28.8% of the total variance and exhibits a meridional dipole pattern with large anomalies distributed to the flanks of 20°N. The related time coefficients reveal an obvious interdecadal change, with below-normal values before the early-1990s and above-normal values thereafter (Fig. 10b). In combination with Fig. 10a, it is apparent that the summertime rainfall anomalies during this period are negative over southern India and positive over northern India, presenting a negative–positive meridional dipole pattern from the south to the north of the country. However, from the early-1990s, the distribution of summertime rainfall anomalies is the opposite, with a positive–negative meridional dipole pattern from the south to the north of India.

Meanwhile, the second mode of 9-yr running mean sum-

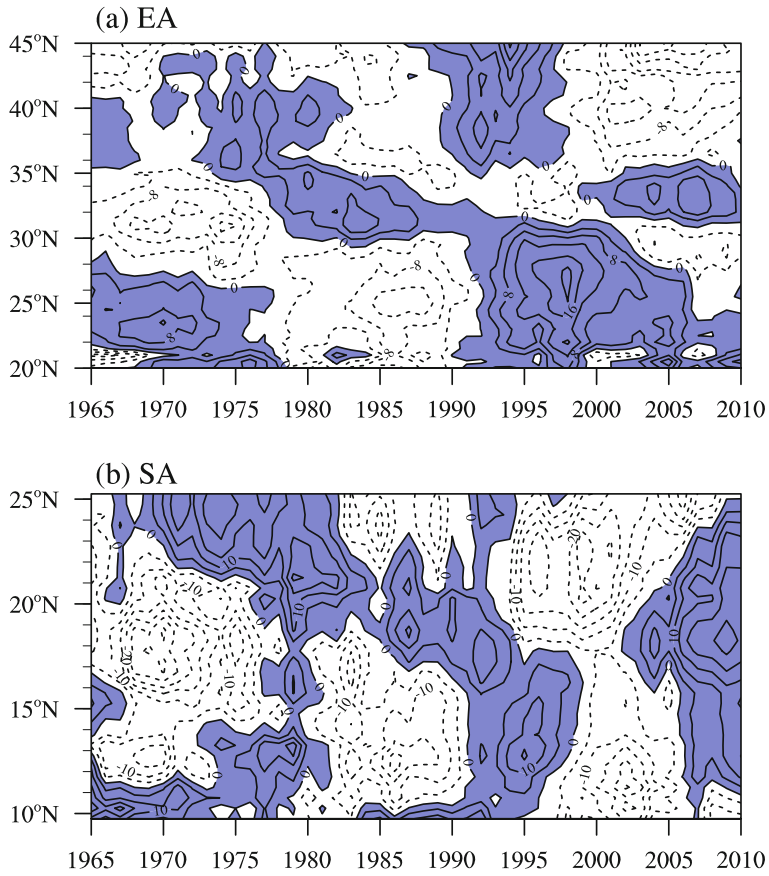

Fig. 9. Latitude–time cross section of 9-yr running mean summertime rainfall anomalies (%) averaged for 100°–120°E in eastern China (a) and for 75°–85°E in the SASM (Indian) region (b). Solid and dashed lines indicate positive and negative anomalies, respectively, and positive anomalies are shaded.

mertime rainfall in the SASM region accounts for 21.8% of the total variance and shows a uniform spatial pattern (Fig. 10c), but with large anomalies to the north of 20°N, which represents a slight southward shift compared with the northern anomalous center in Fig. 10a. The time coefficients are positive prior to the early-1970s and, comparing Figs. 10d and b, the time coefficients of EOF1 are larger than those of EOF2 during this period. Thus, the summertime rainfall anomalies present a negative–positive meridional dipole pattern in India during this period (Fig. 9b). However, from the early-1970s to early-1980s, the time coefficients shown in Fig. 10d change from positive to negative and are larger than those of EOF1 (Fig. 10b); plus, in combination with Fig. 10c, the summertime rainfall anomalies are positive over the whole of India. As for the period from the early-1980s to early-1990s, although the time coefficients of EOF2 are still negative, they are smaller than those of EOF1, and thus the summertime rainfall anomalies also present a negative–positive meridional dipole pattern from the south to the north of India (Fig. 9b). The time coefficients of EOF2 change from negative to positive from the early- to late-1990s. Meanwhile, the time coefficients of EOF1 become positive, and thus the distribution of summertime rainfall anomalies presents a positive–negative meridional dipole pattern from the south to the north of India. As for the period from the late-1990s to the mid-2000s, since the time coefficients of EOF2 are larger than those of EOF1, the distribution of summertime rainfall anomalies thus presents a positive–negative meridional dipole pattern from the south to the north of India.

The 9-yr running mean summertime rainfall anomalous percentages zonally averaged over the domain 75°–85°E are also examined. As shown in Fig. 9b, from the mid-1960s to the early-1990s, the distribution of summertime monsoon rainfall anomalies in the SASM region exhibits a negative–positive meridional dipole pattern from the south to the north of India, except for a positive pattern over the whole of India during the period from the mid-1970s to the early-1980s. From the early- to late-1990s, an opposite anomalous distribution, with a positive–negative meridional dipole pattern from the south to the north of India, appears in this region. Furthermore, during the period from the late-1990s to the mid-2000s, there are negative anomalies over the whole of India. Meanwhile, from the mid-2000s, the summertime rainfall anomalies shift to a positive–negative meridional dipole pattern from the south to the north of India. Besides, the positive and negative anomalies of summertime rainfall in the

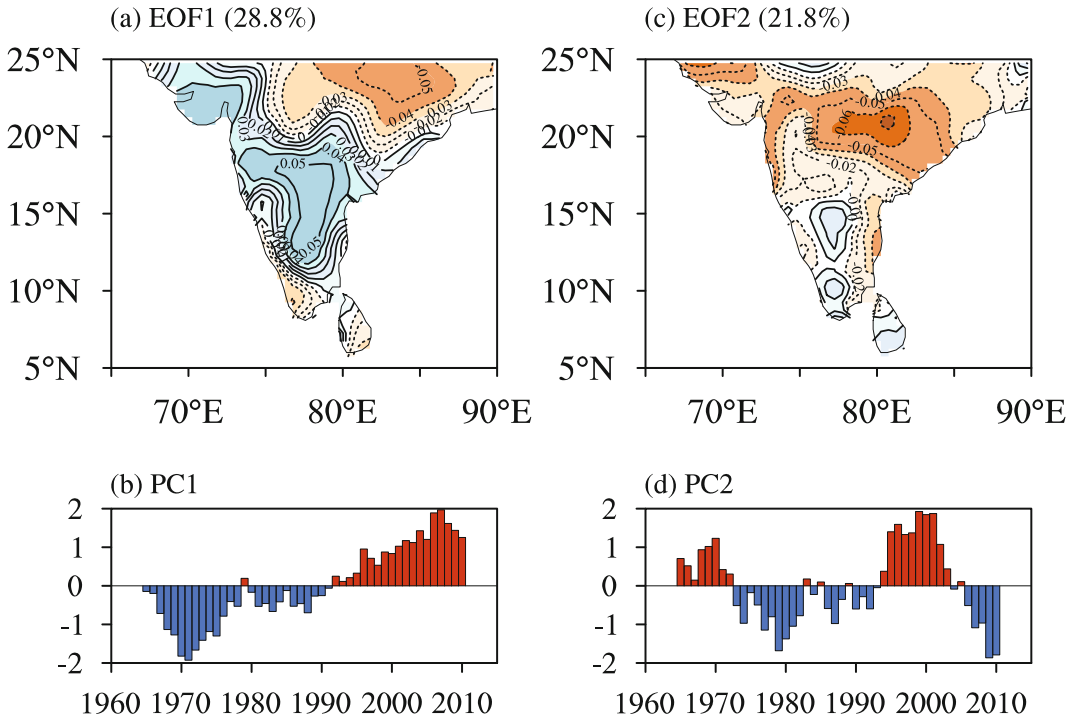

Fig. 10. As in Fig. 8 but for summer rainfall in the SASM (Indian) region. EOF1 and EOF2 explain 28.8% and 21.8% of the total variance, respectively.

SASM region also show a trend of movement from the north to the south.

5.3. *Differences in the characteristics of the interdecadal variability of summertime rainfall in the EASM and SASM regions*

As indicated above, on the interdecadal timescale, the summertime rainfall in both the EASM and SASM regions also show significant differences. The first mode of interdecadal variability of summertime rainfall in both the EASM and SASM regions presents a meridional dipole pattern from the south to the north in its spatial distribution, and both experience an interdecadal variation in the early-1990s. Also, the second mode of the interdecadal variability of summertime rainfall in the EASM region exhibits a tripole structure in spatial pattern and experiences an interdecadal variation in the late-1970s. Meanwhile, the second mode of the interdecadal variability of summertime rainfall in the SASM region shows a uniform spatial pattern and has three interdecadal variations—in the mid-1970s, the early-1990s, and the mid-2000s. Therefore, the interdecadal variability of summertime rainfall in the SASM region may be more complex than that in the EASM region since the early-1990s.

6. Links between the spatiotemporal variabilities of summertime rainfall in the EASM and SASM systems

Although the spatiotemporal variabilities of the EASM system are different from those of the SASM system, there are nevertheless some close links between them. To investigate these links, monsoon indices that measure the strength and variability of the EASM and SASM systems are used to analyze their relationship. Specifically, we use the EAP index to measure the strength of the EASM system, as defined by Huang (2004), and the Webster and Yang (1992) (WY) and Wang and Fan (1999) (WF) indices to measure the strength of the SASM system.

6.1. *Interannual and interdecadal variabilities*

Figure 11 shows the distributions of the linear regression of summertime rainfall anomalies in the EASM and SASM regions with respect to the EAP index, WY index and WF index, separately. Clearly, the regressed rainfall anomalies against the EAP index show a meridional tripole pattern, with negative anomalies in the Yangtze River valley and positive anomalies in North China and the southeastern coast of China (Fig. 11a). This resembles the first mode of summer rainfall in the EASM region and suggests the EAP index describes the interannual variability of the EASM well. The rainfall anomalies over India, regressed against the WY and WF indices, show strong similarities, especially in northern India (Figs. 11b and c); and combining the first mode of summer rainfall in the SASM region, the WF index may be more suitable to measure the variability of the EASM.

There is high correlation between the EAP and WF indices; their correlation coefficient is around 0.32, reaching the 98% confidence level. This high correlation indicates a close link between the first mode of summertime rainfall in the EASM and SASM regions. This link can also be seen from the correlation between the time coefficient series of the

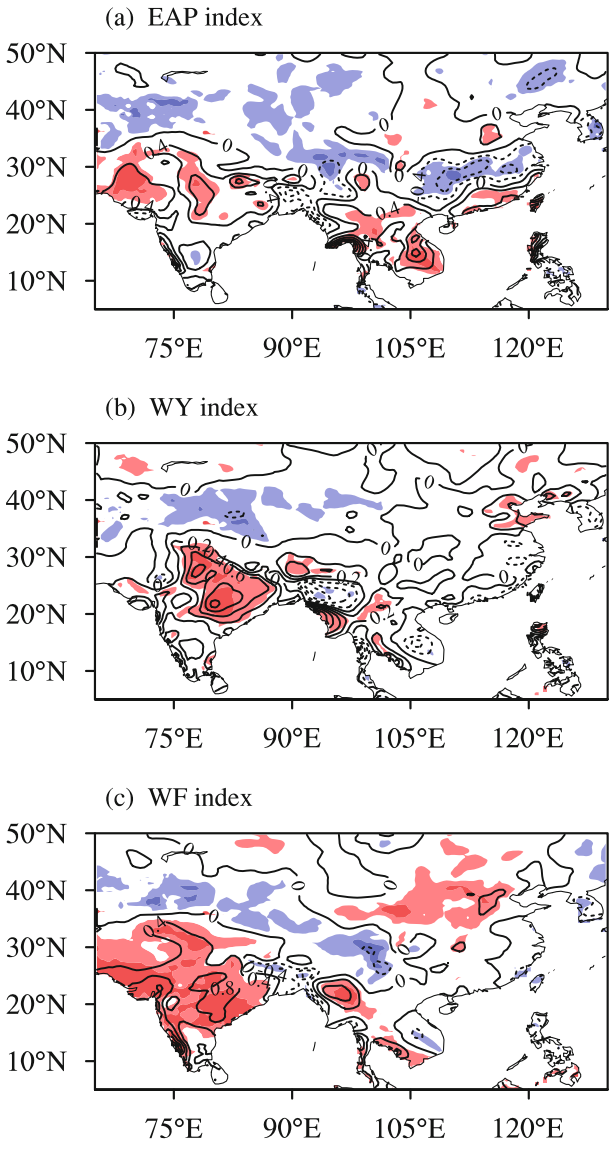

Fig. 11. Linear regression of summertime rainfall anomalies in Eurasia against (a) the EAP index, (b) the WY index and (c) the WF index. Shaded areas denote anomalies exceeding the 95% confidence level.

first mode of summertime rainfall in the EASM and SASM regions. Their correlation coefficient reaches −0.23, which is significant beyond90% confidence level. This means that, if the monsoon rainfall anomaly in India in summer is positive, then it is also positive in South China and North China, while it is negative in the Yangtze River valley. Furthermore, this relationship is unstable, becoming stronger from the early-1990s; the correlation coefficient is only −0.19 during 1961–93, but reaches −0.33 during 1994–2014, at the greater than 90% confidence level. There is also a close link between the interdecadal variability of summertime rainfall in the EASM and SASM regions. The correlation between the first mode of summer rainfall in the EASM and SASM regions reaches −0.58, with statistical significance above the 90% confidence level, suggesting a closer relationship on the interdecadal timescale.

Previous studies have also pointed out the positive correlation between the summertime monsoon rainfall in India and that in North China (Kripalani and Kulkarni, 2001; Wu, 2002, 2017), and that it mainly exists in the quasi-biennial oscillation mode of summertime rainfall in these two monsoon regions (Lin et al., 2016). These studies, however, were based on the correlation between averaged summer monsoon rainfall anomalies over India and North China, which is different to our study. The relationship in the present study is between the first mode of summertime rainfall, with a meridional tripole pattern from the south to the north of eastern China, and the first mode of summertime rainfall, with a uniform pattern in India.

Moreover, it is clear that the regressed rainfall anomalies against the three indices show close similarities over the Eurasian continent. There is a significant meridional teleconnection pattern in the anomalous rainfall from South Asia to North China, showing a positive–negative–positive tripole structure from the south to the north of the Asian summer monsoon region. We refer to this teleconnection as the South Asia/East Asia teleconnection of Asian summer monsoon rainfall anomalies. This agrees with previous findings of a meridional tripole teleconnection existing not only in the EASM, which is related to the Pacific–Japan oscillation, or EAP teleconnection pattern (Nitta, 1987; Huang and Li, 1988; Huang and Sun, 1992), but also in the Asian summer monsoon rainfall anomalies from South Asia to North China (Liu and Ding, 2008; Ding et al., 2013).

6.2. *Spatiotemporal variabilities of summertime water vapor transport*

The close links between the first modes of interannual and interdecadal variability of summertime rainfall in the EASM and the SASM systems may be closely related to the links between the spatiotemporal variabilities of summertime water vapor transport. It is clear from the climatological mean distribution of water vapor transport fluxes over the Asian summer monsoon shown (Fig. 4) that a large amount of water vapor is transported into the EASM region from the Bay of Bengal in summer. Thus, the spatiotemporal variabilities of summertime water vapor transport over the EASM region should be closely associated with those over the SASM region. The correlations between the time-coefficient series of the first two leading modes of summertime water vapor transport fluxes over the EASM and SASM regions are investigated (figure not shown). The correlation coefficients between corresponding pairs are 0.35 and 0.38, respectively, which all reach the 99% confidence level. These correlations can explain the close link between the spatiotemporal variabilities of summertime water vapor transport in the EASM and SASM regions.

7. Conclusions and discussion

Using long-term observational and reanalysis data, the differences and links between the climatological features and interannual/interdecadal variabilities of summer rainfall in

the EASM and SASM regions are analyzed. The main results can be summarized as follows:

The climatological characteristics of summer rainfall in the EASM and SASM regions show obvious differences in terms of the rainfall cloud systems. In the EASM region, there is a mix of stratiform and cumulus rainfall, whereas the SASM is dominated by cumulus cloud systems. This difference may be due to the regions' differences in vertical wind shear in the zonal and meridional winds and the convergence of water vapor transport. The contribution of moisture advection and wind convergence to the convergence of the water vapor transport flux are comparable in the EASM region. However, the contribution of wind convergence is superior to that of moisture advection in the SASM region.

The first two leading modes of the spatiotemporal variabilities of summertime rainfall in the EASM and SASM regions exhibit remarkable interannual variability, with quasi-biennial oscillation and interdecadal variability, and obviously different spatial distributions. In the EASM region, the first and second modes of the interannual variability of summertime rainfall present a meridional tripole pattern and meridional dipole pattern, respectively. Meanwhile, those in the SASM region present a uniform pattern and meridional dipole pattern, respectively. Furthermore, on the interdecadal timescale, the first and second modes of summertime rainfall in the two monsoon regions are similar in pattern to the second and first modes of their interannual variability in their spatial distributions, respectively.

The variability of the summer rainfall in the EASM and SASM regions shows close links on both the interannual and interdecadal timescale. The first mode of interannual variability of summer rainfall in the two monsoon regions has a high negative correlation, and this relationship becomes stronger from the early-1990s. Furthermore, on the interdecadal timescale, the first modes of the summer rainfall in the two monsoon regions also have a high negative correlation. This high correlation of summer rainfall in the EASM and SASM regions may be linked by a meridional tripole teleconnection pattern from South Asia to North China, through the southeast part of the Tibetan Plateau, in the regressed summertime rainfall anomalies over the Asian summer monsoon regions, which agrees with previous studies (Liu and Ding, 2008; Ding et al., 2013). We refer to this pattern as the South Asia/East Asia teleconnection of Asian summer monsoon rainfall.

Overall, it is clear that there are some close links between the EASM and SASM systems, but that the summertime rainfall cloud systems and the spatiotemporal variabilities of summertime rainfall in the EASM region are different from those in the SASM region. Therefore, the EASM system may be a relatively independent monsoon subsystem linked closely to the SASM system in the Asian–Australian monsoon system. Also, it should be pointed out that many problems remain regarding our understanding of the basic physical processes involved in the differences and links between the EASM and SASM systems, and these need to be urgently studied in future work. In particular, the thermal effect of the western Pacific warm pool and the tropical Indian Ocean on the spatiotemporal variabilities of the EASM and SASM systems and their links should be systematically investigated.

Acknowledgements. This study was supported jointly by the National Key Research and Development Program (Grant No. 2016YFA0600603), the National Basic Research of China (Grant No. 2013CB430201) and the National Natural Science Foundation of China (Grant Nos. 41605058, 41375065, 41461164005, 41230527, and 41375082).

REFERENCES

Cheng, A. N., W. Chen, and R. H. Huang, 1998: The sensitivity of numerical simulation of the East Asian monsoon to different cumulus parameterization schemes. *Adv. Atmos. Sci.*, **15**, 204–220, doi: 10.1007/s00376-998-0040-6.

Davis, R. E., 1976: Predictability of sea surface temperature and sea level pressure anomalies over the North Pacific Ocean. *J. Phys. Oceanogr.*, **6**, 249–266, doi: 10.1175/1520-0485(1976)006<0249:POSSTA>2.0.CO;2.

Deng, W. T., Z. B. Sun, G. Zeng, and D. H. Ni, 2009: Interdecadal variation of summer precipitation pattern over eastern China and its relationship with the North Pacific SST. *Chinese Journal of Atmospheric Sciences*, **33**, 835–846, doi: 10.3878/j.issn.1006-9895.2009.04.16. (in Chinese)

Ding, Q. H., and B. Wang, 2005: Circumglobal teleconnection in the Northern Hemisphere summer. *J. Climate*, **18**, 3483–3505, doi: 10.1175/JCLI3473.1.

Ding, Y. H., 2007: The variability of the Asian summer monsoon. *J. Meteor. Soc. Japan*, **85B**, 21–54, doi: 10.2151/jmsj.85B.21.

Ding, Y. H., Z. Y. Wang, and Y. Sun, 2008: Inter-decadal variation of the summer precipitation in East China and its association with decreasing Asian summer monsoon. Part I: Observed evidences. *International Journal of Climatology*, **28**, 1139–1161, doi: 10.1002/joc.1615.

Ding, Y. H., and Coauthors, 2013: Interdecadal and interannual variabilities of the Asian summer monsoon and its projection of future change. *Chinese Journal of Atmospheric Sciences*, **37**, 253–280, doi: 10.3878/j.issn.1006-9895.2012.12302. (in Chinese)

Fu, Y. F., Y. H. Lin, G. S. Liu, and Q. Wang, 2003: Seasonal characteristics of precipitation in 1998 over East Asia as derived from TRMM PR. *Adv. Atmos. Sci.*, **20**, 511–529, doi: 10.1007/BF02915495.

Guo, Q. Y., 1992: Teleconnection between the floods/droughts in North China and Indian summer monsoon rainfall. *Acta Geographica Sinica*, **47**, 394–402, doi: 10.11821/xb199205002. (in Chinese)

Guo, Q. Y., and J. Q. Wang, 1988: A comparative study on summer monsoon in China and India. *Journal of Tropical Meteorology*, **4**, 53–60. (in Chinese)

Halverson, J. B., T. Rickenbach, B. Roy, H. Pierce, and E. Williams, 2002: Environmental characteristics of convective systems during TRMM-LBA. *Mon. Wea. Rev.*, **130**, 1493–1509, doi: 10.1175/1520-0493(2002)130<1493:ECOCSD>2.0.CO;2.

Harris, L., P. D. Jones, T. J. Osborn, and D. H. Lister, 2014: Updated high-resolution grids of monthly climatic observations-

the CRU: TS3.10 Dataset. *International Journal of Climatology*, **34**, 623–642, doi: 10.1002/joc.3711.

Huang, G., 2004: An index measuring the interannual variation of the East Asian summer monsoon-The EAP index. *Adv. Atmos. Sci.*, **21**, 41–52, doi: 10.1007/BF02915679.

Huang, G., Y. Liu, and R. H. Huang, 2011a: The interannual variability of summer rainfall in the arid and semiarid regions of northern China and its association with the Northern Hemisphere circumglobal teleconnection. *Adv. Atmos. Sci.*, **28**(2), 257–268, doi: 10.1007/s00376-010-9225-x.

Huang, R. H., 2006: Progresses in research on the formation mechanism and prediction theory of severe climatic disasters in China. *Advances in Earth Science*, **21**, 564–575, doi: 10.11867/j.issn.1001-8166.2006.06.0564.

Huang, R. H., and W. J. Li, 1988: Influence of the heat source anomaly over the tropical western Pacific on the subtropical high over East Asia and its physical mechanism. *Chinese Journal of Atmospheric Sciences*, **12**, 107–116, doi: 10.3878/j.issn.1006-9895.1988.t1.08. (in Chinese)

Huang, R. H., and F. Y. Sun, 1992: Impacts of the tropical western Pacific on the East Asian summer monsoon. *J. Meteor. Soc. Japan*, **70**, 243–256, doi: 10.2151/jmsj1965.70.1B_243.

Huang, R. H., and L. T. Zhou, 2002: Research on the characteristics, formation mechanism and prediction of severe climatic disasters in China. *Journal of Natural Disasters*, **11**, 1–9, doi: 10.3969/j.issn.1004-4574.2002.01.001. (in Chinese).

Huang, R. H., Y. H. Xu, P. F. Wang, and L. T. Zhou, 1998a: The features of the catastrophic flood over the Changjiang River basin during the summer of 1998 and cause exploration. *Climatic and Environmental Research*, **3**, 300–313, doi: 10.3878/j.issn.1006-9585.1998.04.02. (in Chinese)

Huang, R. H., Z. Z. Zhang, G. Huang, and B. H. Ren, 1998b: Characteristics of the water vapor transport in East Asian monsoon region and its difference from that in South Asian monsoon region in summer. *Scientia Atmospherica Sinica*, **22**, 460–469, doi: 10.3878/j.issn.1006-9895.1998.04.08. (in Chinese)

Huang, R. H., Y. H. Xu, and L. T. Zhou, 1999: The interdecadal variation of summer precipitations in China and the drought trend in North China. *Plateau Meteorology*, **18**, 465–476, doi: 10.3321/j.issn:1000-0534.1999.04.001. (in Chinese).

Huang, R. H., G. Huang, and Z. G. Wei, 2004: Climate variations of the summer monsoon over China. *East Asian Monsoon*, C. P. Chang, Ed., World Scientific Publishing Co. Pte. Ltd., 213–270.

Huang, R. H., R. S. Cai, J. L. Chen, and L. T. Zhou, 2006a: Interdecadal variations of drought and flooding Disasters in China and their association with the East Asian climate system. *Chinese Journal of Atmospheric Sciences*, **30**, 730–743, doi: 10.3878/j.issn.1006-9895.2006.05.02. (in Chinese)

Huang, R. H., J. L. Chen, G. Huang, and Q. L. Zhang, 2006b: The quasi-biennial oscillation of summer monsoon rainfall in China and its cause. *Chinese Journal of Atmospheric Sciences*, **30**, 545–560, doi: 10.3878/j.issn.1006-9895.2006.04.01. (in Chinese)

Huang, R. H., L. Gu, L. T. Zhou, and S. S. Wu, 2006c: Impact of the thermal state of the tropical western Pacific on onset date and process of the South China Sea summer monsoon. *Adv. Atmos. Sci.*, **23**, 909–924, doi: 10.1007/s00376-006-0909-1.

Huang, R. H., J. L. Chen, and G. Huang, 2007: Characteristics and variations of the East Asian monsoon system and its impacts on climate disasters in China. *Adv. Atmos. Sci.*, **24**, 993–1023, doi: 10.1007/s00376-007-0993-x.

Huang, R. H., L. Gu, J. L. Chen, and G. Huang, 2008: Recent progresses in studies of the temporal-spatial variations of the East Asian monsoon system and their impacts on climate anomalies in China. *Chinese Journal of Atmospheric Sciences*, **32**, 691–719, doi: 10.3878/j.issn.1006-9895.2008.04.02. (in Chinese)

Huang, R. H., J. L. Chen, and Y. Liu, 2011b: Interdecadal variation of the leading modes of summertime precipitation anomalies over eastern China and its association with water vapor transport over East Asia. *Chinese Journal of Atmospheric Sciences*, **35**, 589–606, doi: 10.3878/j.issn.1006-9895.2011.04.01. (in Chinese)

Huang, R. H., J. L. Chen, L. Wang, and Z. D. Lin, 2012: Characteristics, processes, and causes of the spatio-temporal variabilities of the East Asian monsoon system. *Adv. Atmos. Sci.*, **29**, 910–942, doi: 10.1007/s00376-012-2015-x.

Huang, R. H., Y. Liu, and T. Feng, 2013: Interdecadal change of summer precipitation over Eastern China around the late-1990s and associated circulation anomalies, internal dynamical causes. *Chinese Science Bulletin*, **58**, 1339–1349, doi: 10.1007/s11434-012-5545-9.

Kalnay, E., and Coauthors, 1996: The NCEP/NCAR 40-year reanalysis project. *Bull. Amer. Meteor. Soc.*, **77**, 437–471, doi: 10.1175/1520-0477(1996)077<0437:TNYRP>2.0.CO;2.

Kripalani, R. H., and S. V. Singh, 1993: Large scale aspects of India-China summer monsoon rainfall. *Adv. Atmos. Sci.*, **10**, 71–84, doi: 10.1007/BF02656955.

Kripalani, R. H., and A. Kulkarni, 2001: Monsoon rainfall variations and teleconnections over South and East Asia. *International Journal of Climatology*, **21**, 603–616, doi: 10.1002/joc.625.

Krishnamurti, T. N., and Y. Ramanathan, 1982: Sensitivity of the monsoon onset to differential heating. *J. Atmos. Sci.*, **39**, 1290–1306, doi: 10.1175/1520-0469(1982)039<1290:SOTMOT>2.0.CO;2.

Kwon, M. H., G. J. Jhun, and K. J. Ha, 2007: Decadal change in East Asian summer monsoon circulation in the mid-1990s. *Geophys. Res. Lett.*, **34**, L21706, doi: 10.1029/2007GL031977.

Lin, D. W., C. Bueh, and Z. W. Xie, 2016: Relationship between summer rainfall over North China and India and its genesis analysis. *Chinese Journal of Atmospheric Sciences*, **40**, 201–214, doi: 10.3878/j.issn.1006-9895.1503.14339. (in Chinese)

Liu, P., and Y. F. Fu, 2010: Climatic characteristics of summer convective and stratiform precipitation in southern China based on measurements by TRMM precipitation radar. *Chinese Journal of Atmospheric Sciences*, **34**, 802–814, doi: 10.3878/j.issn.1006-9895.2010.04.12. (in Chinese)

Liu, Y., G. Huang, and R. H. Huang, 2011: Inter-decadal variability of summer rainfall in Eastern China detected by the Lepage test. *Theor. Appl. Climatol.*, **106**(3–4), 481–488, doi: 10.1007/s00704-011-0442-8.

Liu, Y. Y., and Y. H. Ding, 2008: Analysis and numerical simulation of the teleconnection between Indian summer monsoon and precipitation in North China. *Acta Meteorologica Sinica*, **66**, 789–799, doi: 10.11676/qxxb2008.072. (in Chinese)

McBride, T. L., 1987: The Australian summer monsoon. *Monsoon Meteorology*, C. P. Chang and T. N. Krishnamurti, Eds., Oxford University Press, 203–232.

Nitta, T., 1987: Convective activities in the tropical western Pacific and their impact on the Northern Hemisphere summer circulation. *J. Meteor. Soc. Japan*, **64**, 373–390, doi:

10.2151/jmsj1965.65.3_373.

North, G. R., T. L. Bell, R. F. Cahalan, and F. J. Moeng, 1982: Sampling errors in the estimation of empirical orthogonal functions. *Mon. Wea. Rev.*, **110**(7), 699–706, doi: 10.1175/1520-0493(1982)110<0699:SEITEO>2.0.CO;2.

Staff Members of the Section of Synoptic and Dynamic Meteorology, Institute of Geophysics and Meteorology, Academia Sinica, 1957: On the general circulation over Eastern Asia (I). *Tellus*, **9**, 432–446, doi: http://dx.doi.org/10.1111/j.2153-3490.1957.tb01903.x.

Staff Members of the Section of Synoptic and Dynamic Meteorology, Institute of Geophysics and Meteorology, Academia Sinica, 1958a: On the general circulation over Eastern Asia (II). *Tellus*, **10**, 58–75, doi: 10.1111/j.2153-3490.1958.tb01985.x.

Staff Members of the Section of Synoptic and Dynamic Meteorology, Institute of Geophysics and Meteorology, Academia Sinica, 1958b: On the general circulation over Eastern Asia (III). *Tellus*, **10**, 299–312, doi: 10.1111/j.2153-3490.1958.tb02018.x.

Tao, S. Y., and L. X. Chen, 1987: A review of recent research on the East Asian summer monsoon in China. *Monsoon Meteorology*, C. P. Chang and T. N. Krishnamurti, Eds., Oxford University Press, 60–92.

Tropical Rainfall Measuring Mission (TRMM), 2011: TRMM_3A25: TRMM Precipitation Radar Rainfall L3 1 month (5 x 5) and (0.5 x 0.5) degree V7. Greenbelt, MD, Goddard Earth Sciences Data and Information Services Center (GES DISC), Accessed https://disc.gsfc.nasa.gov/datacollection/TRMM_3A25_7.html.

Wang, B., and Z. Fan, 1999: Choice of South Asian summer monsoon indices. *Bull. Amer. Meteor. Soc.*, **89**, 629–638, doi: 10.1175/1520-0477(1999)080<0629:COSASM>2.0.CO;2.

Wang, B., R. G. Wu, and K.-M. Lau, 2001: Interannual variability of the Asian summer monsoon: Contrasts between the Indian and the western North Pacific-East Asian monsoons. *J. Climate*, **14**, 4073–4090, doi: 10.1175/1520-0442(2001)014<4073:IVOTAS>2.0.CO;2.

Wang, L., and W. Gu, 2016: The Eastern China flood of June 2015 and its causes. *Science Bulletin*, **61**, 178–184, doi: 10.1007/s11434-015-0967-9.

Webster, P. J., and S. Yang, 1992: Monsoon and ENSO: Selectively interactive systems. *Quart. J. Roy. Meteor. Soc.*, **118**, 877–926, doi: 10.1002/qj.49711850705.

Webster, P. J., V. O. Magaña, T. N. Palmer, J. Shukla, R. A. Tomas, M. Yanai, and T. Yasunari, 1998: Monsoons: Processes, predictability, and the prospects for prediction. *J. Geophys. Res.*, **103**, 14 451–14 510, doi: 10.1029/97JC02719.

Wu, R. G., 2002: A mid-latitude Asian circulation anomaly pattern in boreal summer and its connection with the Indian and East Asian summer monsoons. *International Journal of Climatology*, **22**, 1879–1895, doi: 10.1002/joc.845.

Wu, R. G., 2017: Relationship between Indian and East Asian summer rainfall variations. *Adv. Atmos. Sci.*, **34**, 4–15, doi: 10.1007/s00376-016-6216-6.

Wu, R. G., Z. P. Wen, S. Yang, and Y. Q. Li, 2010: An Interdecadal Change in Southern China Summer Rainfall around 1992/93. *J. Climate*, **23**, 2389–2403, doi: 10.1175/2009JCLI3336.1.

Yasunari, T., and R. Suppiah, 1988: Some problems on the interannual variability of Indonesian monsoon rainfall. *Tropical Rainfall Measurements*, J. C. Theon and N. Fugono, Eds., Deepak, Hampton, 113–122.

Yeh, T. C., and P. C. Chu, 1958: *Some Fundamental Problems of the General Circulation of the Atmosphere*. Science Press, Beijing, 159 pp. (in Chinese)

Yeh, T. C., S. Y. Tao, and M. T. Li, 1959: The abrupt change of circulation over the Northern Hemisphere during June and October. *The Atmosphere and the Sea in Motion*, B. Bolin, Ed., The Rockefeller Institute Press and Oxford University Press, 249–267.

Yeh, T. C., 2008: *Selected Papers of Ye Duzheng*. Anhui Educational Publishing House, 498pp. (in Chinese)

Zhang, R. H., 2015: Changes in East Asian summer monsoon and summer rainfall over eastern China during recent decades. *Science Bulletin*, **60**, 1222–1224, doi: 10.1007/s11434-015-0824-x.

Zhao, G. J., G. Huang, R. G. Wu, W. C. Tao, H. N. Gong, X. Qu, and K. M. Hu, 2015: A new upper-level circulation index for the East Asian summer monsoon variability. *J. Climate*, **28**, 9977–9996, doi: 10.1175/JCLI-D-15-0272.1.